Spin-orbit torque controlled MTJ with low thermal stability for tunable random number generation

Vaibhav Ostwal, Joerg Appenzeller

School of Electrical and Computer Engineering & Birck Nanotechnology Center, Purdue University, West Lafayette, IN-47907, United States

Abstract: Spin-orbit torque has emerged as an alternative to Spin-transfer torque switching of thermally stable Magnetic Tunnel Junctions (MTJs). For MTJs with low thermal stability, i.e. low energy barrier MTJs, spin-orbit torque devices have been proposed, which allow for tunable Random Number Generation and decoupled WRITE and READ paths. Such stochastic devices can then be interconnected to realize computational systems, such as Ising networks, neural networks, invertible logic etc. In this article, we experimentally demonstrate such a stochastic spin device called a "p-bit", which is characterized by a spin-orbit torque controlled MTJ with low thermal stability as WRITE unit, and where the tunneling magnetoresistance is employed as READ unit. We first demonstrate deterministic switching of stable in-plane MTJs using the spin-orbit torques generated by Tantalum. Next, we employ spin-orbit torques to tune the stochasticity of the MTJ with low thermal stability to generate tunable random numbers. National Institute of Standards and Technology (NIST) randomness tests are performed to evaluate the quality of our random number generator. The results are then quantitatively analyzed using the standard model for thermally activated switching and the theory of thermal fluctuation in superparamagnetic particles. The devices presented in this work consisting of a WRITE path (spin-orbit torque) and a READ path (MTJ) are the key building blocks for probabilistic spin logic applications.

I. INTRODUCTION

For conventional memory applications, thermally stable MTJs with energy barriers, E_b > 40 kT resulting in years of retention time are desired. MTJs with low E_b on the other hand show random telegraphic "hopping" between their <+m> and <-m> magnetization states in the time domain[1]. Such telegraphic hopping can be tuned with an external magnetic field to achieve a tunable Random Number Generator (RNG) [1]. In this way the binary stochastic behavior of MTJ with low thermal stability can become an asset to solve computational problems, which are difficult to solve using conventional CMOS switches[2][3][4][5]. However, for such computational systems, electrical rather than magnetic field control over the telegraphic switching is desired, where an electrical input controls the amount of time the MTJ with low thermal stability is in its <+m> and <-m> state. By controlling the probability of the <+m> and <-m> state, we can mimic binary stochastic neurons, which can output either a 0 or a 1 with the probability "p" controlled by the input, resulting in a sigmoidal activation function. One of the proposed spin devices called "p-bit" uses spin currents generated by spin Hall effect (SHE) to control (WRITE) the stochasticity of MTJ with low thermal stability[5]. In this device design, WRITE and READ paths are decoupled as reading of the MTJs is performed by the current flowing through the MTJ, while the write current is passed through a heavy metal with giant SHE (GSHE), such as Tantalum[5][6]. By using 3-terminal SOT devices in the p-bit configuration, input-output isolation can be achieved similar to the situation in field effect transistor devices where the input-gate is isolated from the output-drain. Interconnected networks of such spin-orbit torque (SOT) controlled low barrier MTJs are capable of performing Boolean and more-than-Boolean computation, such as invertible logic[5], Ising networks for

optimization problems[4], and Bayesian networks[7]. Implementations of neuromorphic systems[6][8][9], sensor applications[10] and analog to digital converters [11] have also been proposed using such SOT devices.

In this article, we first demonstrate deterministic SOT switching of thermally stable in-plane MTJs using Ta. Next, we will discuss the telegraphic switching of an MTJ with low thermal stability and estimate its dwell time and energy barrier. We have employed the NIST Statistical Test Suit (STS) [12] to evaluate the quality of our RNGs. High quality random numbers are needed for encryption algorithms[13][14] and Monte-Carlo simulations[15]. A previous approach [16] to generate random numbers used stable MTJs and disturb pulses to achieve a 50% switching probability. However, to generate random numbers using MTJs with low thermal stability, no disturb pulses are required. High operational speeds as reported in [16] can be achieved with our approach as thermally driven random hopping can occur on nanosecond time scales for low enough energy barriers as shown from sLLG equation simulations [5][6]. In section III, we first use magnetic fields to control the stochasticity of the MTJ and then show SOT control of the MTJ with low thermal stability by means of a DC current passing through a Ta layer controlling the time the system stays in its <+m> and <-m> state.. Table 1 lists various approaches used in previous studies and our approach to achieve a tunable RNG using SOT devices. An experimental demonstration of SOT controlled MTJ with low thermal stability, as demonstrated here, is a major step towards realization of probabilistic computing with 3-terminal spin devices.

	STT based Tunable RNG	SOT based Tunable RNG
High energy barrier nanomagnets	In-plane MTJ [17][18]: • Source for random hopping: opposing nature of STT and external magnetic fields	nanomagnets with PMA [19]: • Source for random hopping: metastable state induced in PMA with SOT
Low energy barrier nanomagnets	In-plane MTJ [1]: • Source for random hopping: Thermal noise • Tuning of the random hopping: Spin-transfer torque (STT)	In-plane MTJ [this article]: • Source for random hopping: Thermal noise • Tuning of the random hopping: SOT

Table 1: Previously explored spin devices to generate random hopping using either stable or unstable nanomagnet

II. EXPERIMENTAL METHODS

An MTJ stack of Ta/CoFeB/MgO/CoFeB/Ru/CoFe/ PtMn/Ru (fig 1(a)) was sputtered onto a Si/SiO_2 substrate using the Singulus Tool at SUNY ALBANY, where the CoFeB/Ru/CoFe stack acts as a synthetic anti ferromagnetic (SAF) fixed layer, while PtMn is an antiferromagnetic layer coupled to the SAF by means of exchange interaction. This stack is similar to the magnetic stack used in STT-MTJs with exchange coupled SAF as fixed layer[20][21], with the difference, however, that for our SOT-MTJs, the free layer CoFeB is located at the bottom of the stack, with a 5 nm Ta layer underneath[22]. MTJs were pattered using a two-step e-beam lithography approach and Ar ion-milling. In the 1st lithography step, the bottom electrode was patterned by etching down to the substrate, while in the second lithography step, the MTJ metal pillar was defined by etching until the bottom Ta layer was reached. The width and length of the Ta-channel are around 3 um and 12 um

respectively. Elliptical MTJs were patterned such that their easy axis is aligned perpendicular to the current flow direction in the Ta underlayer to ensure that no symmetry breaking magnetic field was required for SOT switching[23][24]. 90 nm of SiO_x is used to electrically isolate the top and the bottom contact of the MTJs. Finally, contacts were formed using a lift-off process. MTJs were annealed at 300° C for an hour in a low-pressure Helium environment in the presence of an in-plane magnetic field of 1 T collinear with easy axis of the MTJs. DC current pulses or constant DC currents are used for SOT control of the MTJs with a measurement set-up as shown in fig1(b). Tunneling Magneto Resistance (TMR) was measured directly across the MTJ using an AC current of 2 μA at a frequency of 497 Hz employing lock-in technique with time constants of 10 ms as shown in fig 1(b).

III. RESULTS AND DISCUSSION

SOT switching of a thermally stable MTJ (device 1):

TMR vs. B-field major and minor loops of a thermally stable MTJ (device 1) (size~260*400 nm^2) are shown in fig 1(c). Information about the field sweep rate is provided in the figure caption. The minor loop for

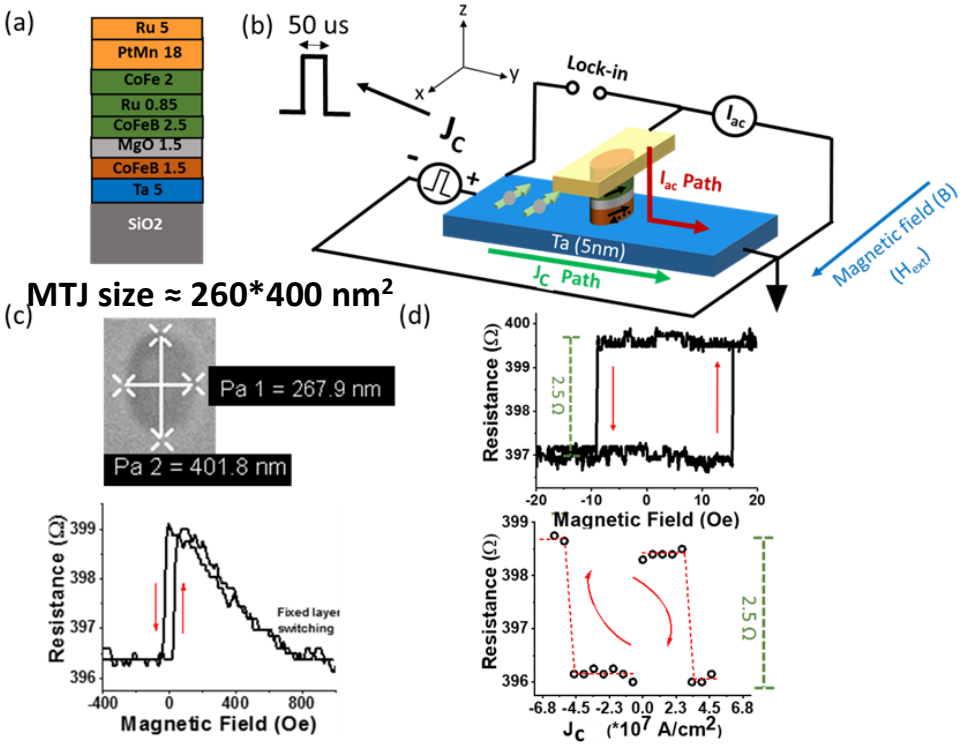

Fig 1 (a) Material stack for our SOT-MTJ (b) MTJ measurement set-up for SOT switching (c) Scanning Electron Microscope (SEM) image of the MTJ and major loop for TMR vs. magnetic field (sweep rate = 480 Oe/min) of device 1 (d) Minor loop (sweep rate = 40 Oe/min) and SOT switching of stable MTJ with quasi-static current pulses (50 μs wide) showing AP to P switching for positive and P to AP switching for negative current pulses.

this device size exhibits an offset of ~4 Oe. As apparent from the major loop, the MTJ gradually settles to the P state at magnetic fields of around 1000 Oe due to the exchange coupled SAF switching, which is similar to STT-MTJs with exchange coupled SAF layer[21]. Note that our MTJs exhibit relatively low TMR and resistance-area products due to unintentional side wall metal re-deposition during the etching of our MTJ pillars[25]. This side-wall metal re-deposition around the MTJ structures shunts the current from flowing through the tunneling barrier and thus reduces the TMR signal. Figure S1 in the supplementary information shows the major loop of a large MTJ of size 10*25 $μm^2$ to illustrate that the low TMR persists even for larger MTJs. Next, we used the GSHE in Ta to switch the magnetization of the free CoFeB magnetic layer of the MTJ

by passing quasi-static current pulses of 50 μs in width through the Ta bottom layer. Fig. 1(d) shows GSHE current switching in the presence of an in-plane field of 4 Oe to compensate for the small offset observed in the minor B-field loop. The current density is calculated assuming that all current is passing through the 5 nm thick Ta with a channel width of 3 um. In the measurement set-up, positive currents will generate spins in the -x direction and hence a low-resistance parallel (P) state will be preferred by the system. Note that positive current pulses will create positive Oersted fields, and these Oersted fields will try to switch the MTJ to its high-resistance anti-parallel (AP) state. Hence, Oersted fields due to the applied current pulses can be excluded as the reason for the observed MTJ switching. In other words, the polarity of the switching in our experiment is consistent with the expected GSHE effect stemming from the current through Ta. For AP to P switching, the current density required is around $3.5*10^7$ A/cm^2, while P to AP switching requires a current density of around $4.5*10^7$ A/cm^2. Fig S3 in the supplementary information shows repeated measurements of magnetic field minor loops and SOT switching of the thermally stable device 1. To evaluate these numbers, we are calculating the intrinsic critical current density required for GSHE switching according to [26]:

$$J_{c0} = (\frac{2q}{\hbar})\mu_0 M_s t\alpha(H_k^{in-plane} + \frac{M_s}{2})\frac{1}{\Theta_{SHE}} \qquad \text{…equation (1)}$$

where M_s is the saturation magnetization moment (≈1100 emu/cc) [22], t is the thickness of the magnet (1.5 nm), α is the damping constant (0.01)[1], $H_k^{in-plane}$ is the in-plane anisotropy field and Θ_{SHE} is the spin Hall angle of Ta (≈0.1)[27]. For the in-plane magnet, the $H_k^{in-plane}$ term can be neglected compared to $\frac{M_s}{2}$ (especially for MTJs with low aspect ratio as used in our experiments). From these numbers we obtain $J_{c0} = 3.46 * 10^7 \frac{A}{cm^2}$ from eq. (1). Considering the quasi-static (pulsed) switching we employed in our experiments, the critical current J_c can be calculated using the standard model for thermally activated switching [25] [26]:

$$J_c = J_{c0}\left[1 - \frac{k_B T}{E_b}\ln\frac{\tau}{\tau_0}\right] \qquad \text{….equation (2)}$$

where τ_0 is the attempt time (≈1ns) and τ is the pulse width of the GSHE current used (50 μs). For stable MTJs assuming $\frac{E_b}{k_B T} = 40$, J_c is approximately $0.75*J_{c0} = 2.58 * 10^7 \frac{A}{cm^2}$. This value is in good agreement with our experimental findings, considering that any Oersted fields will oppose the SOT switching. We also note that these switching current densities are similar to those previously reported for in-plane MTJs[22][28].

SOT control of MTJ with low thermal stability (device 2):

Having demonstrated GSHE switching in thermally stable MTJs, we will next discuss similar measurements performed on a second type of MTJ, which has low thermal stability. The size of this MTJ is around 160*260 nm^2 as apparent from the SEM shown in the figure 2(a), and its smaller size is responsible for the different behavior if compared to device 1. During a slow magnetic field sweep near the minor loop this MTJ toggles between two states (AP and P), exhibiting telegraphic behavior as shown in figure 2(a). A major loop measurement is included in the supplementary information (fig S2) showing gradual magnetization switching of the reference layer similar to device 1 at magnetic fields of 100 mT. The offset in the minor loop

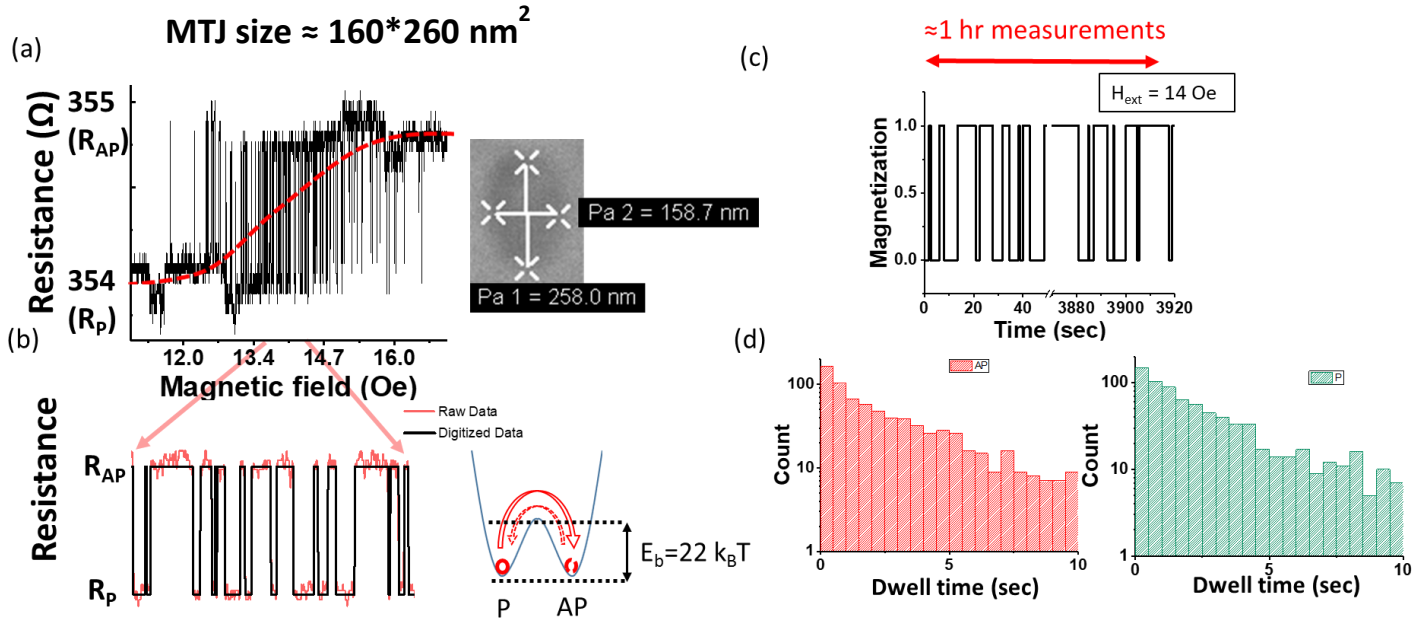

Fig 2 (a) Minor B-field loop (sweep rate= 0.4 Oe/min) for a MTJ with low thermal stability (device 2) with the SEM image. When the B-field is swept slowly during the minor loop measurement, the MTJ with low thermal stability shows random fluctuations between the AP and P states. The minor loop offset is around 14 Oe for this device size. (b) Zoom-in minor loop at H_{ext} of 14 Oe (to compensate for the minor loop offset at zero magnetic field) showing telegraphic switching between the AP and the P state (red curve) and digitized data (black curve) to infer the magnetization state of the free layer. (c) Magnetization states obtained when measuring for ~1hr at H_{ext}=14 Oe. (d) number of counts vs. dwell time obtained for AP (Red) and P (Green) states in a semi-logarithmic plot using the measurement in (c). At H_{ext} = 14Oe, this MTJ shows equal characteristic lifetimes for the AP and P state.

for this device size is around 14 Oe, which is a result of stray fields from the SAF or Neel dipolar orange-peel effect [1]. Fig. 2 (b) shows a zoom-in image of the minor loop at around 14 Oe with two distinct resistance states AP and P respectively. Note that the black line is a digitized version of the raw data. The sweep rate used for the minor loop measurement was 0.4 Oe/min. The MTJ under investigation is in its P state for magnetic fields < 10 Oe and in its AP state for fields > 17 Oe. Random telegraphic switching between the AP and P state is expected to follow a Poisson distribution with respect to the dwell time, i.e. the time the MTJ stays in either of the two states and should exponentially decrease. To perform such a dwell time analysis, the MTJ resistance was characterized for over an hour at an external field of 14 Oe. Next, the magnetoresistance data are digitized to +1 and 0 by applying a proper threshold operation to the TMR data as displayed in figure 2(b). At an external field of 14 Oe, the probability for the MTJ to be in its AP versus P state is found to be ~50 %. Figure 2(d) displays the number of counts for a dwell time in a semi-logarithmic plot. From the linear fit to this plot a

characteristic lifetime to find the MTJ in its P (τ_P) and AP (τ_{AP}) state of around 3 sec is found for both τ_P and τ_{AP}. Using this experimental finding, an energy barrier ($\Delta_{in-plane}$) of ~22 k_BT can be determined from $\tau = \tau_0 exp\left[\frac{\Delta_{in-plane}}{k_BT}\right]$. Fig S4 in the supplementary information shows telegraphic switching of the device 2 for external fields of 14 Oe at 290 K, 300 K and 320 K showing the expected temperature dependence in switching rates.

Next, tests from the National Institute of Standards and Technology (NIST) Statistical Test Suit (STS) [12] are performed based on the above experimental magnetization data that was used for the dwell time analysis. Since, $\tau_P = \tau_{AP}$ = 3 sec, magnetization states are read after each 6 sec (2τ) for the NIST tests. Note that some of the tests in the suit are not applicable due to the limited sample size (~650 samples) in our case. Table 2 shows the test name and the respective p-values obtained for the test on the raw data and after performing an XOR operation used to increase the Shannon entropy [29] and hence the randomness. If the obtained p-value is greater than 0.01, the sample is considered to have passed the test. As shown in table 2, already the raw data obtained from the magnetization states of our stochastic, i.e. MTJ with low thermal stability passes all the test performed (shown in green) except one (shown in red), while data after XOR operations passes all the randomness tests performed.

Randomness test name	P-value without XOR	P-value after XOR
Frequency test	0.272095	0.753684
Frequency test within block	0.651978	0.938924
Runs test	0.659677	0.100225
Longest runs test	0.002909	0.628936
Binary matrix rank test	0.375518	0.834948
Discrete Fourier transform	0.652767	0.087321
Serial test 1	0.010302	0.015907
Serial test 2	0.034779	0.068169
Approximate Entropy test	0.028691	0.025147
Cumulative sums test forward	0.509393	0.315833
Cumulative sums test backward	0.155112	0.168758

Table 2: NIST STS randomness test and results (p-values) obtained from measuring the MTJ with low thermal stability at 14 Oe (sample size~650 samples If a p-value greater than 0.01 is obtained, the test has been successfully passed.

As discussed before, both: i) magnetic fields and ii) SOT can deterministically switch high barrier nano-magnets (see discussion around figure 1). In the case of MTJ with low thermal stability, magnetic fields and SOT are thus expected to tune the probability of a low barrier MTJ to be found in its AP or P state. To increase the speed of telegraphic switching the temperature was raised to 320 K in this experiment. Next, the MTJ resistance was monitored while passing a DC current ranging from -250 µA to 200 µA through the Ta layer in the presence of a magnetic field of 14 Oe to compensate for the offset of the minor loop. Further optimization of the SAF layer will be required to remove such offset in the minor loop and achieve field-free operation in the future. The telegraphic switching of this MTJ for different DC currents flowing through the Ta layer is shown in figure 3(a). The voltage drop across the MTJ is not affected by the DC currents flowing through the Ta layer due to the three-terminal nature of SOT devices. Only currents flowing through the MTJ

determine the voltage drop across the MTJ, which is essential for a proper implementation of p-bits [5]. For positive DC currents the MTJ prefers to stay in its P state while negative DC currents result in a higher probability to find the system in its AP state. This preference is consistent with the deterministic switching of thermally stable magnets (see figure 1(d)) and agrees with the sign of the SOT generated by the Ta. Again, note that Oersted fields would result in exactly the opposite tuning compared to the SOT by the Ta layer.

Last, we want to compare our experimental results on the SOT impact with the expectation to find the system as a function of the current through the Ta layer in its AP state. For this, the resistance values obtained for various DC currents were digitized, and the probability of the MTJ to be in its AP state is calculated from the experimental data. Figure 3(b) shows this probability as a function of the amount of current flowing through the Ta Hall bar structure, clearly showing a sigmoidal shape, which starts saturating around 250 μA. This current corresponds to a density of $1.7*10^6$ A/cm^2. For MTJ with low thermal stability, the characteristic lifetime of the P or AP state in the presence of a spin current is given by[1][30],

$$\tau_{P,AP} = \tau_0 exp\left[\frac{\Delta_{in-plane}}{k_B T}\left(1 \mp \frac{J}{J_{c0}}\right)\right] \quad \text{....equation (3)}$$

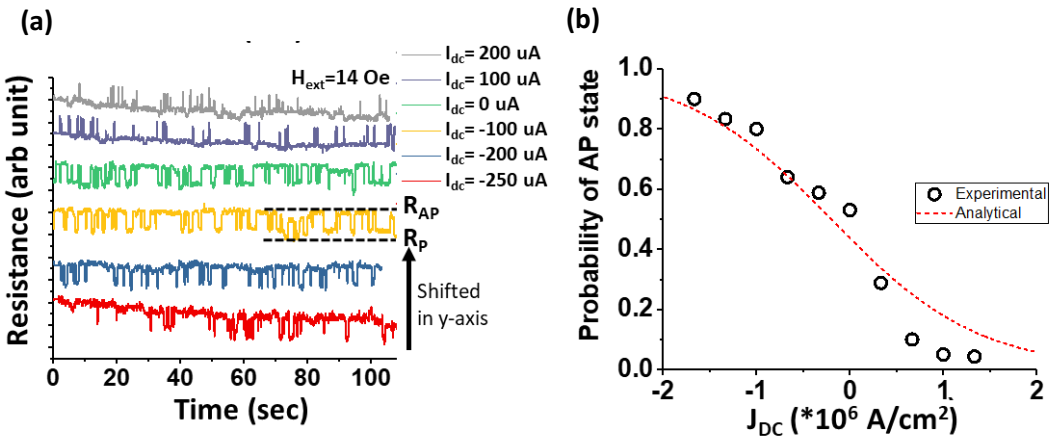

Fig 3 (a) MTJ with low thermal stability resistance data showing telegraphic switching between the AP and P state for H_{ext} = 14 Oe and different I_{dc} flowing through the GSHE Ta layer. (b) The probability for the MTJ with low thermal stability to be found in its AP state versus current density flowing through Ta (black circles) based on data from (a) and expected probability obtained using the analytical expression eq. 3 (red curve)

where J_{c0} is the characteristic critical current density $J_{c0} = 3.46 * 10^7 \frac{A}{cm^2}$, which was calculated before, while $\Delta_{in-plane}$=22*k_BT. Hence, for the input current density J, the probability to find the MTJ in its AP state is given by $\frac{\tau_{AP}}{\tau_P+\tau_{AP}}$. The sigmoidal curve obtained from this analysis is plotted in figure 3(b) and matches closely the experimentally obtained data. Some of the parameters used for the analytical fit, such as the spin Hall angle or the damping constant are taken from the literature, which reports substantial variations of these values. While a better analytical fit to our presented measured data can in principle be obtained (as shown in supplementary information fig S5) by using different sets of parameters, our limited data set size prohibits currently the extraction of more detailed information.

CONCLUSION

In the post-Moore Law era, tunable RNG is an essential capability to build many of the more-than-Boolean computing systems. MTJs with low thermal stability are natural candidates as RNG, while spin-currents can be used in an efficient way to tune such MTJs and hence provide a compact device that is capable to operate as a tunable RNG. In this article, we have shown that SOTs can tune MTJ with low thermal stability in a "single device geometry", in this way creating a compact tunable RNG. Compared to STT controlled, SOT controlled MTJ with low thermal stability provide the additional advantage of decoupled WRITE and READ paths. Our demonstration is a step towards realization of novel computing systems with so-called "p-bits" with characteristics of input-output isolation and tunable random number generation.

REFERENCES

[1] M. Bapna and S. A. Majetich, "Current control of time-averaged magnetization in superparamagnetic tunnel junctions," *Appl. Phys. Lett.*, vol. 111, 243107, 2018.

[2] A. Mizrahi *et al.*, "Neural-like computing with populations of superparamagnetic basis functions," *Nat. Commun.*, vol. 9, 1533, 2018.

[3] S. Ganguly, K. Y. Camsari, and A. W. Ghosh, "Reservoir Computing using Stochastic p-Bits," *arXiv: 1709.10211*, 2017.

[4] B. Sutton, K. Y. Camsari, B. Behin-aein, and S. Datta, "Intrinsic optimization using stochastic nanomagnets," *Sci. Rep.*, vol. 7, 44370, 2017.

[5] K. Y. Camsari, R. Faria, B. M. Sutton, and S. Datta, "Stochastic p-bits for invertible logic," *Phys. Rev. X*, vol. 7, 031014 , 2017.

[6] C. M. Liyanagedera, A. Sengupta, A. Jaiswal, and K. Roy, "Stochastic Spiking Neural Networks Enabled by Magnetic Tunnel Junctions : From Nontelegraphic to Telegraphic Switching Regimes," *Phys. Rev. Appl.*, vol. 8, 064017, 2017.

[7] R. Faria, K. Y. Camsari, and S. Datta, "Implementing Bayesian networks with embedded stochastic MRAM," *AIP Adv.*, vol. 8, 045101,2018.

[8] R. Zand, K. Y. Camsari, S. D. Pyle, I. Ahmed, C. H. Kim, and R. F. Demara, "Low-Energy Deep Belief Networks Using Intrinsic Sigmoidal Spintronic-based Probabilistic Neurons," *Proc. 2018 Gt. Lakes Symp. VLSI*, pp. 15–20, 2018.

[9] V. Ostwal, P. Debashis, R. Faria, Z. Chen, and J. Appenzeller, "Spin-torque devices with hard axis initialization as Stochastic Binary Neurons," *Sci. Rep.*, vol. 8, 16689, 2018.

[10] A. Sengupta, C. M. Liyanagedera, B. Jung, and K. Roy, "Magnetic Tunnel Junction as an On- Chip Temperature Sensor," *Sci. Rep.*, vol. 7, 11764, 2017.

[11] A. Agrawal and K. Roy, "Design of a Low-Voltage Analog-to-Digital Converter Using Voltage-Controlled Stochastic Switching of Low Barrier Nanomagnets," *IEEE Magn. Lett.*, vol. 9, pp. 1-5, 2018.

[12] L. E. Bassham *et al.*, "A statistical test suite for random and pseudorandom number generators for cryptographic applications," *Spec. Publ. (NIST SP) - 800-22 Rev 1a*, 2010.

[13] Mathew S K, Srinivasan S, Anders M A, Kaul H, Hsu S K, Sheikh F, Agarwal A, Satpathy S, Krishnamurthy R K (2012), "2.4 Gbps, 7 mW all-digital PVT-variation tolerant true random number generator for 45 nm CMOS high-performance microprocessors," *IEEE J. Solid-State Circuits*, vol. 47, no. 11, pp. 2807–2821,

[14] C. Tokunaga, D. Blaauw, and T. Mudge, "True Random Number Generator With a Metastability-Based Quality Control," *IEEE J. Solid-State Circuits*, vol. 43, pp. 78–85, 2008.

[15] R. Y. Rubinstein, *Simulation and the Monte Carlo Method*, 2nd Edition. John Wiley, 2008.

[16] W. H. Choi *et al.*, "A Magnetic Tunnel Junction based True Random Number Generator with conditional perturb and real-time output probability tracking," *Tech. Dig. - Int. Electron Devices Meet. IEDM*, p. 12.5.1-12.5.4, 2015.

[17] B. R. Zink, Y. Lv, and J. P. Wang, "Telegraphic switching signals by magnet tunnel junctions for neural spiking signals with high information capacity," *J. Appl. Phys.*, vol. 124, 152121, 2018.

[18] R. H. Koch, J. A. Katine, and J. Z. Sun, "Time-Resolved Reversal of Spin-Transfer Switching in a Nanomagnet," *Phys. Rev. Lett.*, vol. 92, 088302, 2004.

[19] D. Bhowmik, L. You, and S. Salahuddin, "Spin hall effect clocking of nanomagnetic logic without a magnetic field," *Nat. Nanotechnol.*, vol. 9, no. 1, pp. 59–63, 2014.

[20] R. Stearrett *et al.*, "Influence of exchange bias on magnetic losses in CoFeB/MgO/CoFeB tunnel junctions," *Phys. Rev. B - Condens. Matter Mater. Phys.*, vol. 86, 014415, 2012.

[21] Y. M. Lee, J. Hayakawa, S. Ikeda, F. Matsukura, and H. Ohno, "Giant tunnel magnetoresistance and high annealing stability in CoFeB/MgO/CoFeB magnetic tunnel junctions with synthetic pinned layer," *Appl. Phys. Lett.*, vol. 89, 042506, 2006.

[22] L. Liu, C. Pai, Y. Li, H. W. Tseng, D. C. Ralph, and R. A. Buhrman, "Spin-Torque Switching with the Giant Spin Hall Effect of Tantalum," *Science*, vol. 336, pp. 555–559, 2012.

[23] L. Liu, O. J. Lee, T. J. Gudmundsen, D. C. Ralph, and R. A. Buhrman, "Current-induced switching of perpendicularly magnetized magnetic layers using spin torque from the spin hall effect," *Phys. Rev. Lett.*, vol. 109, 096602, 2012.

[24] S. Fukami, T. Anekawa, C. Zhang, and H. Ohno, "A spin-orbit torque switching scheme with collinear magnetic easy axis and current configuration," *Nat. Nanotechnol.*, vol. 11, pp. 621–625, 2016.

[25] A. V Penumatcha *et al.*, "Spin-torque switching of a nano-magnet using giant spin hall effect Spin-torque switching of a nano-magnet using giant spin hall effect," *AIP Adv.*, vol. 5, 107144, 2015.

[26] J. Z. Sun, "Spin-current interaction with a monodomain magnetic body: A model study," *Phys. Rev. B*, vol. 62, pp. 570–578, 2000.

[27] M. Cecot *et al.*, "Influence of intermixing at the Ta/CoFeB interface on spin Hall angle in Ta/CoFeB/MgO heterostructures," *Sci. Rep.*, vol. 7, 968, 2017.

[28] S. V. Aradhya, G. E. Rowlands, J. Oh, D. C. Ralph, and R. A. Buhrman, "Nanosecond-Timescale Low Energy Switching of In-Plane Magnetic Tunnel Junctions through Dynamic Oersted-Field-Assisted Spin Hall Effect," *Nano Lett.*, vol. 16, pp. 5987–5992, 2016.

[29] C. Shannon, "A mathematical theory of communication," *Bell Syst. Tech. J.*, vol. 27, pp. 379-423, 1948.

[30] W. F. Brown, "Thermal fluctuations of a single-domain particle," *Phys. Rev.*, vol. 130, 1677, 1963.

ACKNOWLEDGEMENT: This work was supported in part by the Center for Probabilistic Spin Logic for Low-Energy Boolean and Non-Boolean Computing (CAPSL), one of the Nanoelectronic Computing Research (nCORE) Centers as task 2759.003 and 2759.004, a Semiconductor Research Corporation (SRC) program sponsored by the NSF through CCF 1739635.